AIAA 80-0812R

Elevated Temperature Structural Testing of Advanced Missiles

O.R. Otto* and G.J. Inukai†
McDonnell Douglas Astronautics Company, St. Louis, Mo.

Structural tests at room and elevated temperature were conducted on a full-scale aft airframe section of the Advanced Strategic Air-Launched Missile. Loads applied at room temperature represented conditions during captive carry and ejection. Test data are shown to agree well with theory. Loads applied at temperatures up to 1200°F represent conditions during ramjet flight. The high heating rates and temperature levels produced unanticipated and invalid response from some instrumentation. These events will be described and procedures for high-temperature testing will be presented. Although limited elevated-temperature test data were obtained, structural verification of the airframe was achieved.

Introduction

DURING the 1970s, technology integration and development studies were performed on the Advanced Strategic Air-Launched Missile (ASALM). The missile is designed for a variety of air-to-ground and air-to-air missions. Its speed and maneuverability produce conditions where high loads and temperatures exist during ramjet flight. Maximum temperatures of approximately 1700°F in the combustor case and 900°F in the outer wall are obtained. Configuration screening studies indicated significant performance (range) advantages for a concept where the aft airframe body, which houses the integral rocket/ramjet engine, also serves as a wraparound fuel tank. However, testing was required to verify the structural and functional performance of this concept. Accordingly, a full-scale aft airframe test article was fabricated and tested. Observations and results of these tests are presented and discussed in this paper.

Test Article Description

The aft airframe test article, shown in Fig. 1, is 97 in. long, 21.5 in. high and is constructed almost entirely of the titanium alloy 6Al-2Sn-4Zr-2Mo-0.1S (Ti-6242S). An Inconel 718 combustor case was installed in the test article during testing to facilitate simulation of engine heating and internal loads distribution. The primary test section includes the flight vehicle power system (FVPS) section and the center fuel tank. The FVPS and center fuel tank sections were chosen as the critical major body components for the structural test because: 1) they are located in the area of maximum body bending, 2) they include the structure for transferring load from the inner wall and combustor to the outer wall, 3) they are located in an area where thermal effects are significant from aerodynamic heating and late flight internal heating from the engine, and 4) the fuel tank is subjected to internal pressurization loads. Successful performance of these critical components would greatly increase confidence in the structural materials and concepts.

Testing Approach and Setup

Structural integrity of the aft airframe test article Fig. 2, was demonstrated by the successful completion of a comprehensive static test program representing various critical load and temperature combinations. Loads were applied to the test article at room temperature to simulate captive carriage, ejection, and tank pressurization conditions. Loads were applied at elevated temperature to simulate ramjet flight conditions. The external surface was heated to simulate aerodynamic heating while the inside surface of the combustor case was heated to simulate ramjet engine operation.

A typical room-temperature structural test setup is shown in Fig. 3. The test article was attached to the test fixture bulkhead at the 11 in. adapter ring (Fig. 1) and cantilevered from the stand. The loading system consisted of four hydraulic actuators supported by the test stand and located at bulkheads. The four actuators were attached to 2 in. wide tension straps contoured to the test article moldline at the four bulkhead locations: missile stations (M.S.) 77, 85, 105, and 154. The actuators were programmed to apply constant ratio loads to the test article. The loading control system was designed such that if the load on any actuator varied more than 5% from its programmed valve, the test would be aborted.

The fuel tank was pressurized with water for room-temperature testing and with nitrogen for elevated-temperature testing. For safety reasons, a pressure relief valve was used to prevent the internal pressure from exceeding 67% of design ultimate pressure.

A quartz heat lamp assembly was used with the setup in Fig. 3 to simulate aerodynamic heating of the outside surface of the airframe for the ramjet flight test conditions. It is shown partially removed from the test article in Fig. 4. The lamp assembly was mounted on rails to permit easy installation over the test article. A quartz heat lamp assembly was also used internally to heat the combustor.

Both heat lamp assemblies were controlled with a thermocouple feedback system. The outer wall was divided into 10 independent control zones around the circumference. Because of axial symmetry, only one control zone was required for the combustor. Each zone contained a sensor thermocouple which monitored zone temperature. Power to the lamps was determined by the temperature of the sensor thermocouples relative to the programmed value. Significant overtemperature conditions were flagged on a real-time data display such that the test engineers could make immediate abort decisions.

Instrumentation

The test article was instrumented to measure strains, deflections, temperatures, and applied loads. Measurements were made at representative points in sufficient quantity and

Presented as Paper 80-0812 at the AIAA/ASME/ASCE/AHS 21st Structures, Structural Dynamics and Materials Conference, Seattle, Wash., May 12-14, 1980; submitted June 10, 1980; revision received Aug. 11, 1981.

*Section Chief—Technology. Member AIAA.
†Senior Engineer—Technology.

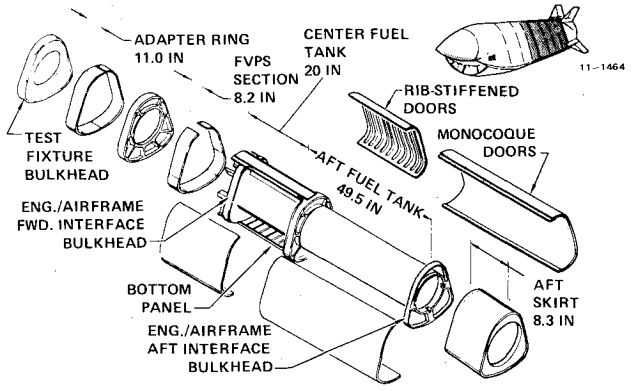

Fig. 1 Major sections of ASALM aft airframe test article.

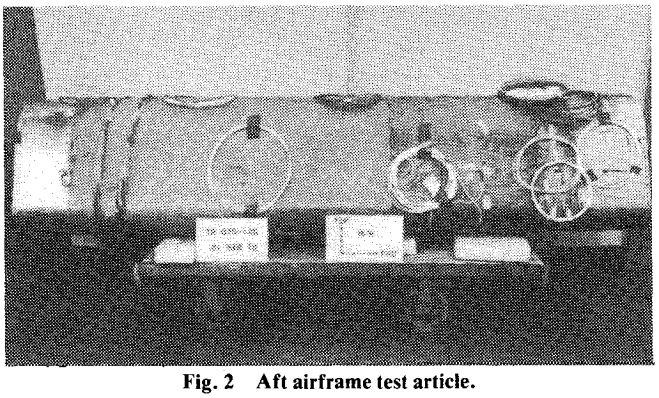

Fig. 2 Aft airframe test article.

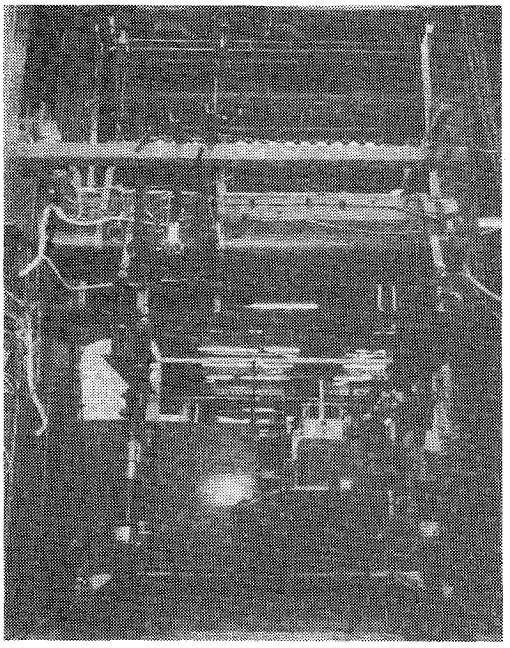

Fig. 3 Test setup to simulate captive carry load condition.

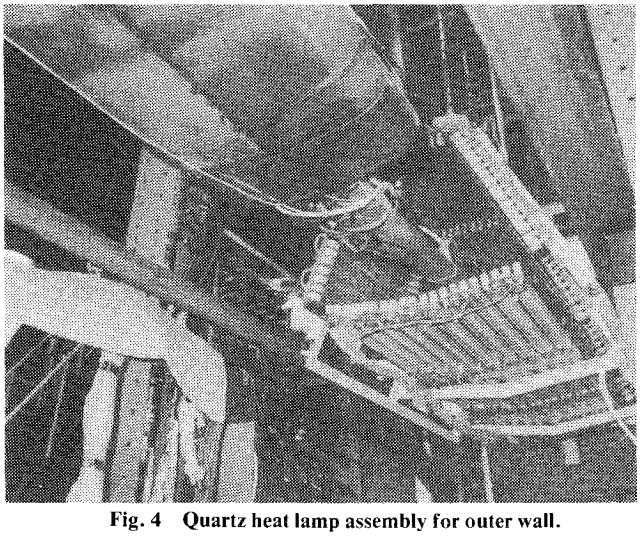

Fig. 4 Quartz heat lamp assembly for outer wall.

accuracy to verify stress analyses, thermal analyses, and deflection predictions. The complete test article was instrumented with 79 strain gages, 92 thermocouples, 6 deflection gages, 1 pressure transducer, and 4 strain links.

Conventional strain gages were used in 54 locations on the test article. They operate satisfactorily up to 500°F for extended periods and at higher temperatures for short periods providing they are bonded with a high-temperature adhesive and cured at a temperature above the temperature at which they are to provide data. Where it was impossible to bond and cure the adhesive directly on the structure, the gage was bonded to 5 mil commercially pure titanium foil which was subsequently poke welded to the component. A typical installation is shown in Fig. 5. Gages were bonded and cured directly to removable components (doors and FVPS panels) in an oven. The gage was sealed from moisture with Silastic DC 3140 and shrink fit tubing (Thermofit MMS 809) was used to protect ends of lead wires where the Teflon insulation was removed. The manufacturer's gage factor and apparent strain data were used to determine elevated temperature strains.

Because structural temperatures for some tests exceeded 500°F, an experimental, free-filament-type strain gage was also used. This experimental gage was reported to have capability for extended operation at temperatures up to 1200°F. Thus, these gages were expected to operate satisfactorily at all elevated temperatures to be experienced by the test article. The test article was instrumented with 25 experimental gages. Several of the experimental gages were located adjacent to conventional gages so that their response characteristics at temperatures below 500°F could be compared directly with the response of proven conventional gages.

Typical installation of the experimental gage is shown in Fig. 6. The gage is attached to a 5 mil thick commercially pure titanium foil with a flame-sprayed ceramic. The ceramic must be thermally conditioned up to 1200°F before repeatable and predictable strains can be measured. Following thermal conditioning, the titanium foil was poke welded to the structure.

One of the disadvantages of this type of gage is the large apparent strain it possesses at elevated temperature as shown in Fig. 7. In addition, apparent strain was found to be quite sensitive to length of lead wire used for the gage. Consequently, it was difficult to accurately measure mechanical strains at elevated temperature using these experimental gages.

Another disadvantage of the experimental strain gage is the large scatter in gage factor as shown in Fig. 8. This scatter is from gage-to-gage readings and from repeated readings of the same gage. Since gage factor relates gage output (millivolts) to strain (inch/inch), variations in gage factor proportionally affect strain accuracies. Differences in gage factor for compression and tension also made data reduction difficult.

Three types of thermocouples were used to obtain thermal response data. Unsheathed chromel/alumel wire thermocouples, designed for temperatures less than approximately 1200°F, were used on the majority of airframe structure. These thermocouples have a felted asbestos, silicon-impregnated glass braid insulation around each conductor, and a stainless-steel braided overwrap. Sheathed chromel/

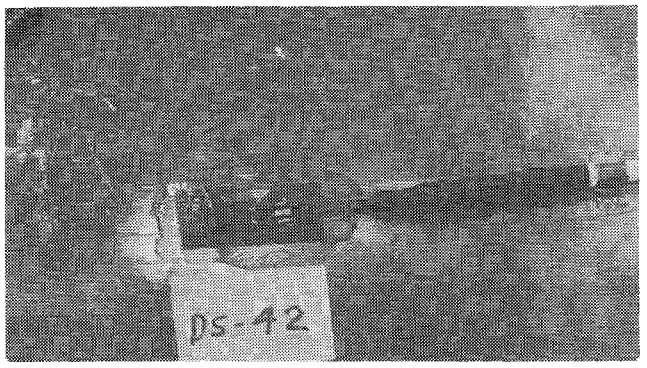

Fig. 5 Conventional strain gage installation.

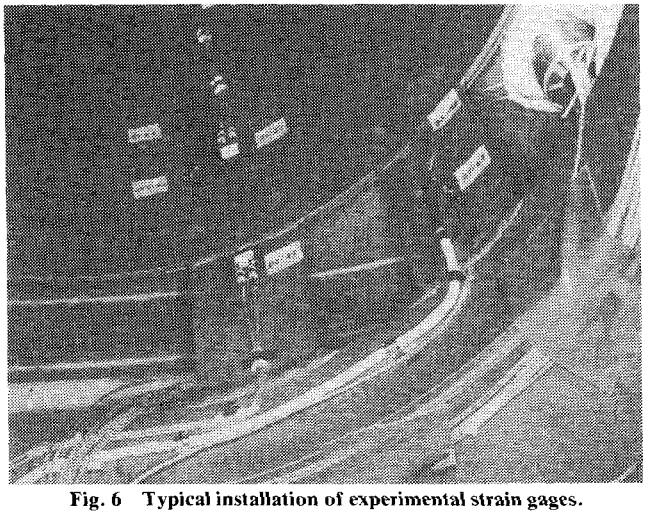

Fig. 6 Typical installation of experimental strain gages.

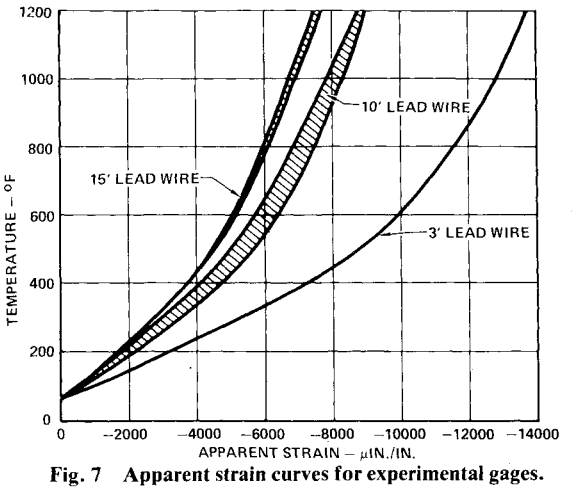

Fig. 7 Apparent strain curves for experimental gages.

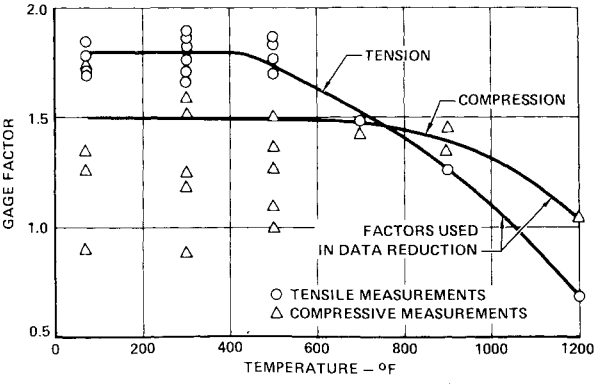

Fig. 8 Gage factor scatter for experimental gages.

alumel wire thermocouples, designed for use at temperatures exceeding 1200°F, were used on the combustor. Gold-plated chromel/alumel thermocouples, designed to measure air temperatures, were located in the load introduction portion of the test article (M.S. 105-154).

Test Program

The structural/thermal test program consisted of six basic tests, shown in Table 1, representing captive carriage, ejection, and ramjet flight conditions. Tests 1-4 represent captive carry and ejection conditions when the airframe maximum temperature is 160°F. These tests were conducted at room temperature because of the negligible difference in strength of titanium structure at 160°F and room temperature. A comparison of missile bending moments for the maximum room-temperature condition and the elevated-temperature ramjet flight conditions is shown in Fig. 9.

Test 5 was conducted at 500°F to insure survival of conventional strain gages and to check out the heating system prior to the high heating rate of test 6. Body bending loads representing a ramjet maneuver condition and fuel tank internal pressure loads were applied after the structure reached 500°F.

Test 6 was planned to represent maneuver loads combined with the maximum temperatures and temperature gradients which occur during a typical long range ramjet flight. The first attempt at test 6 was aborted. The load shown on the lower curve of Fig. 9 was applied and the programmed temperature profile from Fig. 10 was being executed. After 60 sec, the test was aborted because several thermocouples

Table 1 Structural/thermal test conditions

Test	Temperature	Condition	Maximum bending moment, in.-lb	Maximum tank pressure, psig
1	Room	Captive carriage	360,000 (limit)	0
2	Room	Captive carriage	540,000 (ultimate)	38
3	Room	Captive carriage	– 600,000 (ultimate)	0
4	Room	Airlaunch ejection	840,000 (ultimate)	0
4A	Room	Airlaunch ejection	900,000 (ultimate)	0
5	500°F outer wall	Ramjet	530,000 (ultimate)	26
	500°F outer wall	Ramjet	396,000 (ultimate)	0
6	880°F outer wall Room inner wall	Ramjet	175,000 (limit)	26
	700°F outer wall 1000°F inner wall 1500°F combustor	Ramjet	377,000 (ultimate)	0

showed abnormally high temperatures.

Inspection of the test article after the aborted test showed that some instrumentation materials had burned in localized areas during rapid heating to the test condition (Fig. 11). Prior to using these instrumentation materials, they were heated to the elevated temperatures experienced during the test to determine their behavior. However, they were heated slowly and no burning or other anomalies were found.

Several simple experiments were conducted to investigate what may have caused the abnormally high-temperature readings. The experiments indicated that strain gage sealant (Silastic DC 3140), shrink fit tubing (Thermofit MMS 809), and high-temperature strain gage leads (Haskins 875) burned when subjected to test heating rates. It was also found that open-flame heating of the thermocouple leads, such as that caused by burning instrumentation, would cause temperature spikes similar to those experienced during the test.

Prior to completing test 6, conventional strain gage instrumentation was removed and high-temperature strain gage leads were relocated wherever possible. Some temperature spikes from the remaining strain gage instrumentation were still encountered during the completed test 6 run, such as the two shown for zones 2 and 5 in Fig. 10. However, these temporary spikes did not compromise test objectives or data analysis.

After successful completion of test 6, all detachable doors, panels and the combustor were removed. Considerable scaling was found on the fuel tank inner wall as shown in Fig. 12. Chemical analysis indicated over 50% titanium content with smaller amounts of aluminum and tin (components of base metal Ti-6242S). However, ultrasonic measurements of the inner wall indicated less than 0.002 in. loss in material thickness. This material loss has a negligible effect on strength. Several small experiments were conducted to determine the cause of the scale. It was found that the scale was formed by a reaction between the titanium oxide surface and gaseous flourine which forms during the decomposition of Teflon when heated to high temperatures. Teflon was present in the fiberglass cloth facings on the fuel tank insulation and on the strain gage leads located between the inner wall and combustor.

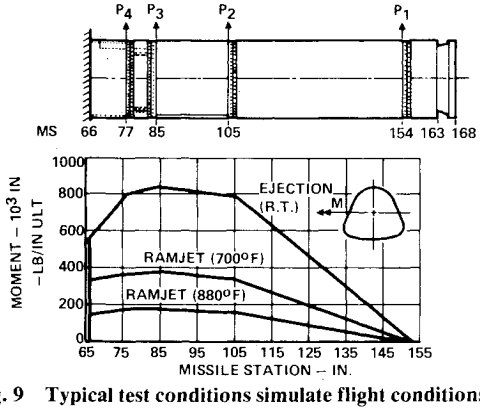

Fig. 9 Typical test conditions simulate flight conditions.

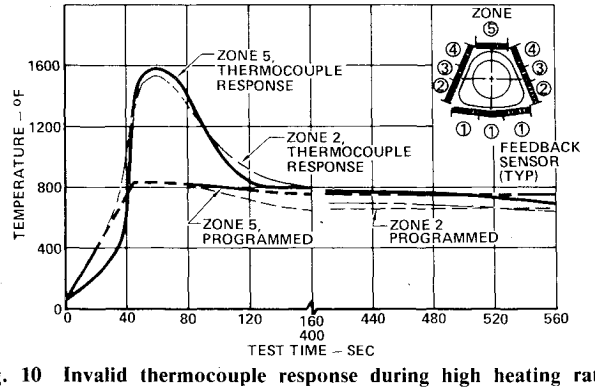

Fig. 10 Invalid thermocouple response during high heating rate structural test.

Test Correlation with Theory

Although some instrumentation difficulties were experienced in the high-temperature tests, valuable data were obtained from all tests for comparison with analytical predictions. Strain gage data obtained in the room-temperature tests were used to verify load sharing of the outer wall, inner wall, and combustor. These components form a redundant structure for carrying body bending loads. Load sharing between the outer wall, inner wall, and combustor was predicted by a NASTRAN finite-element analysis.[1] The elastic model consisted of 1020 nodes and 1400 elements (plates, rods, and bars). Results of the analysis are shown in Fig. 13. Strain gages placed around the circumference of the outer wall, inner wall, and combustor described the strain distribution in each component. Moments carried by each component were determined from the distributions using elementary beam theory. Test results given in terms of percent load carried in each component (Fig. 13) compare well with the NASTRAN predictions.

Results from test 2 were used to investigate the effects of local longitudinal bending strains between the circumferential ribs on the doors and on the bottom panel from internal pressure and longitudinal strains from overall missile body bending. NASTRAN finite-element analyses provided overall

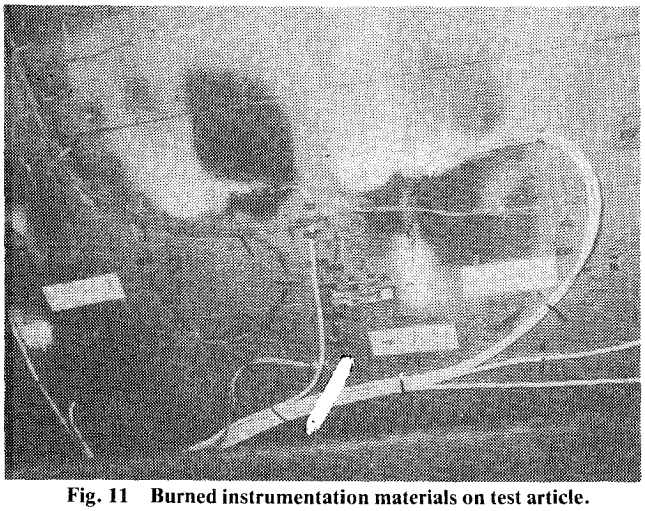

Fig. 11 Burned instrumentation materials on test article.

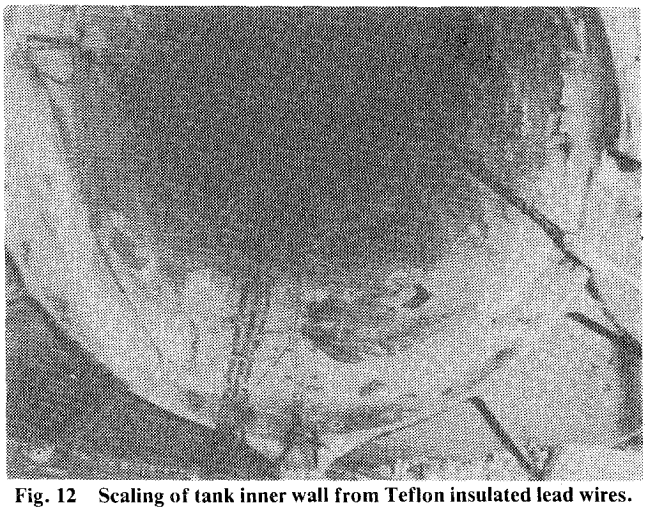

Fig. 12 Scaling of tank inner wall from Teflon insulated lead wires.

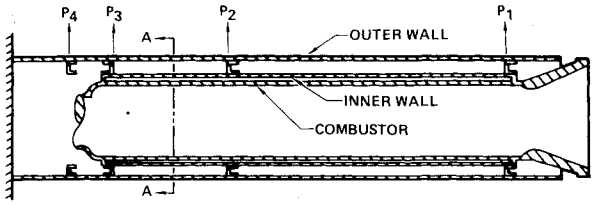

COMPONENT	TEST 3		TEST 4	
	THEORY	TEST	THEORY	TEST
OUTER WALL	69%	70%	72%	70%
INNER WALL	11%	18%	11%	17%
COMBUSTOR	20%	12%	17%	13%
TOTAL MOMENT A–A	–547000 IN–LB		+815000 IN–LB	

Fig. 13 Comparison of load sharing data.

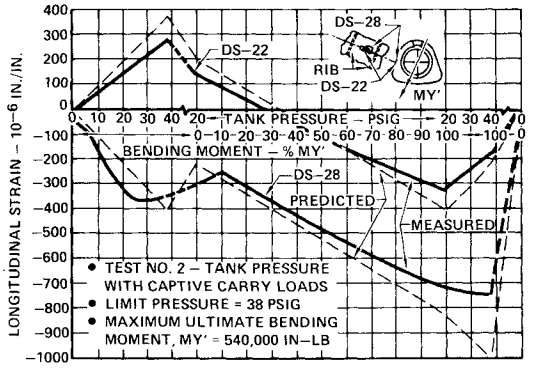

Fig. 14 Longitudinal strains in fuel tank outer wall.

longitudinal and circumferential strains from body bending and internal pressure. Local longitudinal bending strains from internal pressure were calculated considering a longitudinal element between ribs idealized as a plate with fixed ends under conditions of plane strain. The longitudinal strain components were superimposed to determine predicted strains. Figure 14 shows predicted strains on the inside and outside surface of the fuel tank door. The response of two gages measuring longitudinal strains in the fuel tank door at this location are also shown in Fig. 14 for test 2 events. Conventional gage DS-22 was attached to the outside of the door skin between ribs. Conventional gage DS-28 was attached directly opposite on the inside of the skin. These gages combine the local longitudinal bending strains of the skin between the ribs due to internal pressure and the longitudinal compressive strains resulting from captive carry body bending loads. The figure indicates that both gages are measuring strains reasonably close to the predicted values throughout the events of test 2. The nonlinear response and the shift in the knee of the curve of DS-28 during pressurization may be a result of joint slippage, transition from bending to membrane action, or thermal strains induced from the temperature of the water used to pressurize the center fuel tank. No apparent strain corrections were made for this room-temperature test.

Data from test 2 were also used to compare circumferential bending moments in the test article with moments predicted by the NASTRAN finite-element analysis. Circumferential bending is caused almost exclusively by tank pressurization. Figure 15 shows the predicted distribution from NASTRAN analysis for the 38 psig internal pressure used in test 2. Pairs of strain gages, located at four circumferential locations, were used to calculate moments per inch of width in the test article. The calculated moments are also plotted in Fig. 15 and are shown to agree well with the predicted moment distribution.

Fuel tank outer wall deflections due to internal pressure were measured during tests 2, 5, and 6. Results from tests 2 and 5 are compared to deflections predicted by NASTRAN finite-element analyses in Fig. 16. The predicted and measured deflections compare well. Results from test 6 were

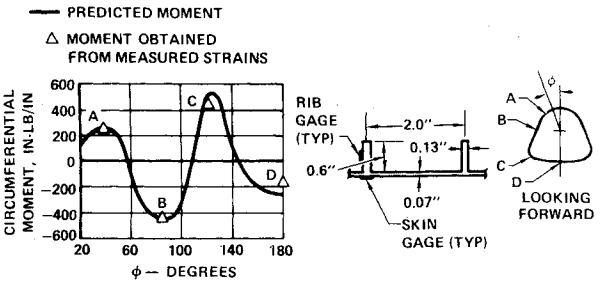

Fig. 15 Predicted bending moments confirmed by test.

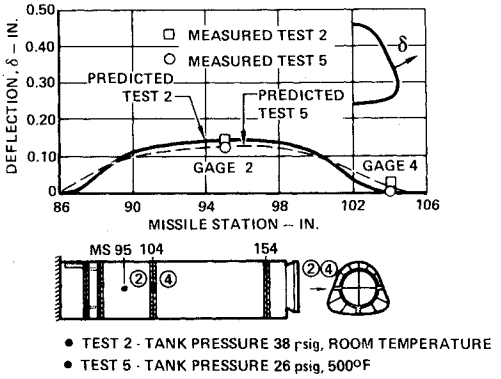

Fig. 16 Fuel tank wall deflections.

similar to those from test 5. The predicted and measured deflections during test 2 result from an internal pressure of 38 psig. Deflections are small near the bulkheads (M.S. 85 and 105) while maximum deflections occur midway between the bulkheads. Deflections during elevated temperature test 5 result from internal pressure of 26 psig and thermal expansion.

Overall body bending deflections were also measured for all tests. As anticipated, the measured deflections were consistently higher than the predicted deflections obtained with the NASTRAN model. The NASTRAN model did not account for the slight slippages in the numerous bolted joints which occurred under load.

Conclusions

The unanticipated response of some instrumentation during these tests convincingly demonstrated the need for careful selection of instrumentation materials which will function properly in the test environment. Instrumentation materials should be checked under actual test conditions. Further development of high-temperature strain gages and attachment approaches is required.

Although some difficulties were experienced with the instrumentation, the overall objectives of the test program were accomplished. Valuable temperature response and deflection data were obtained which were used to validate thermal models and to confirm airframe stiffness predictions. Excellent results were obtained from room-temperature structural tests. Good agreement was found between predicted and measured loads distribution in the airframe components.

Acknowledgments

This paper presents results of structural and thermal tests conducted during the period April 24, 1978 to Aug. 10, 1978 by McDonnell Douglas Astronautics Company—St. Louis, St. Louis, Mo., under Contract F33615-74-C-5175 with the Air Force Aeronautical Systems Division (ASD), Wright-Patterson Air Force Base, Ohio. Lt. Col. Larry Gross (ASD/YYMA) was the Air Force Project Manager.

Reference

[1] "MSC NASTRAN Version 44," Macneal Schwendler Corp., 1978.